



Characterizing multi-phase anomalous gas in galaxies at different stages of infall into the Virgo cluster

PhD research proposal

Sriram Sankar

Supervisors: Prof. Barbara Catinella, Prof. Chris Power

Abstract

Galaxy evolution is primarily driven by the balance between gas accretion and removal processes. Satellites infalling into clusters are subject to numerous environmental gas removal mechanisms that initiate outside-in quenching of the star formation. However, even after the peak of environmental stripping, satellites may retain significant cold gas reservoirs in their inner regions which can fuel star formation for billions of years. To understand the full quenching of star formation, we must resolve and connect multi-phase gas flows in the inner and outer regions of satellites to internal and environmental quenching mechanisms. Non-circular gas flows observed collectively as anomalous gas serve as a robust tracer of both accretion and removal mechanisms. However, our understanding of these remains limited. The ongoing MAUVE (MUSE and ALMA Unveiling the Virgo Environment) survey will provide spatially resolved observations at $\sim 100 - 200$ pc scale for 40 late-type satellites at different stages of infall into the Virgo cluster. As part of my PhD, I will develop techniques to reliably characterise different types of anomalous gas across multiple emission lines, phases, and physical scales. I will then apply these techniques to the MAUVE dataset to investigate the relative impacts of various quenching mechanisms in shaping gas distribution and star formation as a function of galaxy properties and infall time. I will further use mock observations of high-resolution hydrodynamic simulations to examine timescales and pathways of gas depletion and full quenching.

Research project

Galaxies convert less than 20% of their baryons into stars over their lifetimes and hold a substantial fraction of their mass in the surrounding medium, known as the circumgalactic medium (CGM; see left panel of figure 1; [Tumlinson et al. 2017](#)). The CGM plays a critical role in regulating gas flow to and from the interstellar medium (ISM) of galaxies. The ISM and CGM form significant gas reservoirs that can sustain star formation for extended periods. Decades of research on the transition of galaxies from star-forming to quenched populations have established that these gas reservoirs must be affected to halt star formation (see [Cortese et al. 2021](#) for a review). Galaxy evolution is primarily driven by the balance between gas accretion and removal processes. However, our understanding of gas accretion mechanisms is incomplete (e.g. [Afruni et al. 2021, 2023](#)), and the relative impacts of intrinsic versus environmental gas removal processes remain unclear (e.g. [Cortese et al. 2021](#)).

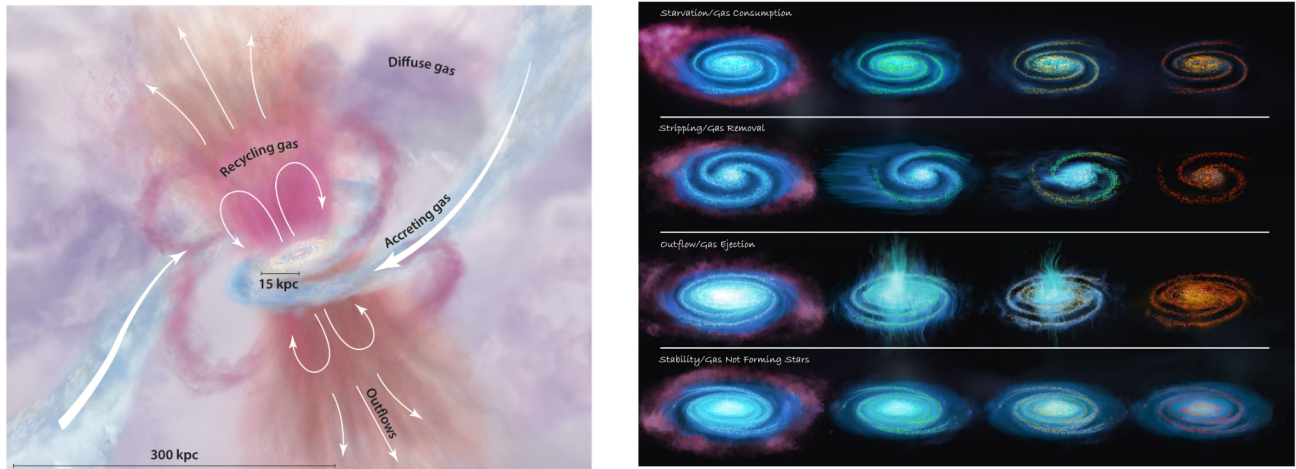


Figure 1: *Left:* A cartoon of the CGM from [Tumlinson et al. \(2017\)](#) representing different gas phases and processes shaping them labelled. *Right:* An illustration of various gas removal and quenching pathways in satellites from [Cortese et al. \(2021\)](#). The ISM is shown in blue and the CGM in pink

Several physical mechanisms have been invoked to explain gas supply in star-forming galaxies and gas removal in galaxies undergoing quenching. It is now evident that these mechanisms differ between central and satellite galaxies, and that a combination of processes is needed to sustain star formation as well as to fully quench galaxies (see right panel of figure 1). High spatial and spectral resolution spectroscopic observations enable us to distinguish non-circular gas flows, such as inflows and outflows, from the dominant differential rotation within a galaxy's disc. **We refer to these non-circular flows, which deviate from the rotation expected for a thin disc in hydrostatic equilibrium, as anomalous gas. Anomalous gas serves as a robust tracer of gas accretion and removal processes, yet our understanding of these remains limited.** This is predominantly due to its characterisation being restricted to single-phase observations (e.g., HI, H α) of small samples of nearby, typically non-interacting and/or star-forming galaxies (e.g. [Marasco et al. 2019](#); [Reichardt Chu et al. 2024](#)). To construct a coherent picture of gas flows, we must observationally resolve all phases of anomalous gas in galaxies across diverse sets of star formation properties and environments. In tandem, we must leverage observational insights to inform theoretical models of gas processing mechanisms and test their predictions of anomalous gas distributions.

1 Anomalous gas

Historically, anomalous gas in galaxies has been identified morphologically and kinematically in emission and absorption across all phases using numerous techniques. In this work, we focus on anomalous gas with sufficient densities to be mapped by sensitive emission-line observations within the disc-halo interface; the fictitious boundary separating the spherical and cylindrical flows. This definition excludes cold gas clumps found at high-impact parameters in the CGM by absorption line studies of background sources. We briefly discuss different categories of anomalous gas that have been observed in external galaxies, highlighting major inferences and related open questions that we plan on addressing in this work.

1.1 Extraplanar gas (EPG)

EPG has been detected morphologically in edge-on (see figure 2) and kinematically in moderately inclined nearby star-forming galaxies. It extends to at least 1-3 kpc vertically away from the midplane of galaxy discs and is characterised by a rotation velocity that lags behind that of the disc (e.g. Fraternali et al. 2002). The EPG has been characterised in a small number of nearby galaxies in the neutral and ionised phases using resolved interferometric (e.g. Fraternali et al. 2002, 2005; Oosterloo et al. 2007; Boomsma et al. 2008) and optical emission line (e.g. Fraternali et al. 2004; Boettcher et al. 2017, 2019) observations. Recently, Marasco et al. (2019) conducted the first systematic investigation of the neutral EPG in a sample of 15 nearby late-type galaxies. They found that the EPG is ubiquitous, comprising about 10-15% of the total HI mass. It extends to a scale height of 1-3 kpc, with a vertical velocity gradient of approximately $-10 \text{ km s}^{-1} \text{ kpc}^{-1}$ and a global inflow rate of about $20 - 30 \text{ km s}^{-1}$ in both the radial and vertical directions. The ubiquitous presence of such a gas structure, which is not in hydrostatic equilibrium far from the star-forming disc, suggests that additional mechanisms are needed to regenerate and sustain the anomalous gas layer. The neutral EPG is expected to have contributions from multiple sources, including recycled gas from galactic fountains driven by stellar feedback, gas condensing from the halo, and gas stripped from companion galaxies.

On the other hand, the extraplanar diffuse ionised gas (eDIG; or just DIG in some works) is expected to originate from gas entrained in outflows and photoionization of the neutral EPG. However, most studies of the EPG to date have focused on investigating galactic fountain cycles in relatively isolated star-forming galaxies. Thus, the relative

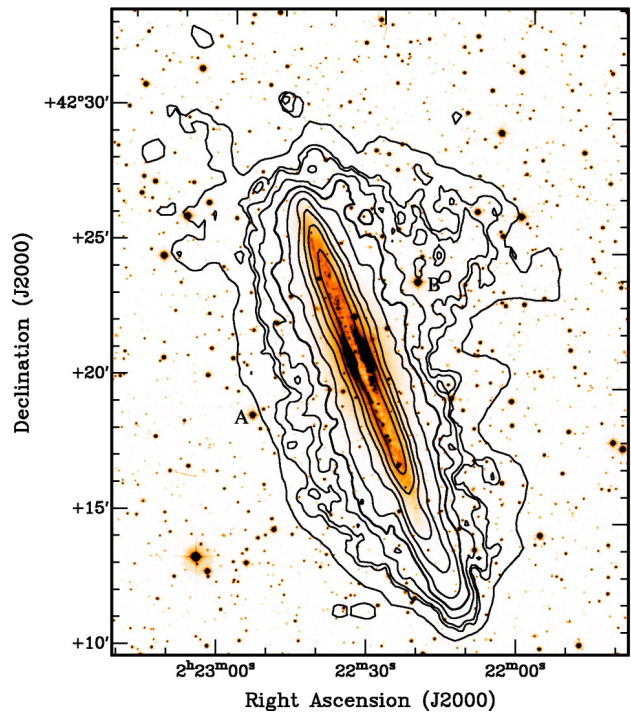


Figure 2: The neutral extraplanar gas layer detected in deep HI 21cm observations of NGC 891 taken from Oosterloo et al. (2007). The HI column density contours are overlaid on an optical image with the lowest level at $5 \times 10^{19} \text{ cm}^{-2}$.

roles of the various plausible mechanisms to dynamically support and replenish the different phases of the EPG remain unconstrained. For instance, recent hot inflow solutions derived by [Stern et al. \(2024\)](#), predict substantial contributions to the EPG from condensation in an inflowing, hot CGM. Such a scenario has not been considered in the past due to assumed hydrostatic equilibrium in the hot halo along the radial and polar directions ([Li et al. 2023](#), Sankar et al. in prep). Furthermore, no work to date has looked at the EPG in galaxies residing in group and cluster environments. Does the EPG survive in satellites infalling to clusters? If not, at what stage does it get stripped? If it is stripped, can galactic fountain cycles replenish the layer and prolong star formation in parts of the disc?

1.2 Outflowing gas

Outflowing gas has been observed in all phases across galaxies at various redshifts, through both emission and down-the-barrel absorption line studies (see reviews by [Veilleux et al. 2020](#) and [Thompson & Heckman 2024](#)). These observations of anomalous gas tracing outflows enable us to probe fundamental aspects of stellar and Active Galactic Nuclei (AGN) feedback, such as kinetic power, momentum rate, and mass loss rate. This, in turn, allows for the direct study of numerous phenomena that shape galaxies, including gas recycling (see [Fraternali 2017](#) and citations therein) and internal quenching mechanisms, including preventive or ejective feedback. However, high-resolution observations of multiple phases at comparable resolutions are required to directly link the observed anomalous gas to the star-formation properties and the underlying multi-scale gas-phase physics. Unfortunately, due to the low surface brightness of outflows, simultaneous resolved observations of all phases of outflows are only available for a few well-known nearby sources with high star formation rates and favourable geometry. In addition, even where outflows are observed, measuring physical parameters is challenging due to projection effects, resolution limitations, and uncertainties in the geometry of the outflow. Thus, the current statistics on outflows are not representative due to most observations being limited to single phases, integrated or stacked galaxy samples or a few nearby starburst galaxies, where outflows are easier to observe ([Veilleux et al., 2020](#); [Reichardt Chu et al., 2024](#)).

Our knowledge of outflows is largely based on observations and models of galaxies with enhanced star formation. It is well established that the observed properties of outflows vary with the gas phase. Evidence from the best-studied outflows in nearby starbursts, M 82 and NGC 253, indicates that while the cold phase ($\leq 10^4$ K) carries most of the mass, the hot phase ($\sim 10^6$ K) holds the majority of the energy (e.g. [Kim et al. 2020](#)). While this behaviour is reproduced in recent ISM patch simulations (see [Li & Bryan 2020](#) for a compilation), it is alarmingly



Figure 3: Ionized gas outflow (red) observed in NGC 4383, overlaid on an optical image. This galaxy is on its first infall to the Virgo cluster. The observation was taken as part of the ongoing MAUVE program ([Watts et al., 2024](#))

different from the predictions of subgrid models typically employed in cosmological simulations. Further, recent numerical and analytical solutions also suggest that the partitioning of mass, momentum, and energy flux between the phases can vary with the height above the midplane and also the initial mass loading of the hot phase (e.g. Schneider et al. 2020; Fielding & Bryan 2022). This calls for re-examining several common assumptions adopted in observations and simulations of galactic outflows. Analytic models provide a useful bridge between observations and simulations. In a series of papers, Orr et al. (2022b,a) introduced, for the first time, a first-principle model that relates local ISM conditions and clustered (spatially and temporally) supernovae (SNe) to the regulation of star formation and the driving of outflows that breakout of the ISM. Their predictions are consistent with the observations of breakout superwinds in local star-forming galaxies (NGC 253 & NGC 4321: Orr et al. 2022a; IRAS 08339+6517: Reichardt Chu et al. 2022). In fact, Orr et al. (2022a) find that in most nearby galaxies, including the Milky Way (solar circle), superbubbles driven by clustered SNe fragment and drive turbulence near the gas disc scale height (≤ 300 pc).

Galaxies that are actively forming stars at a steady rate follow a well-defined relation known as star-forming main sequence (SFMS; e.g. Whitaker et al. 2012). Based on observations of outflows across multiple phases and scale heights in the Milky Way, it is suspected that outflows may be common even in galaxies on or below the SFMS (see section 4.1.1 in Veilleux et al. 2020). However, due to difficulty in recovering subtle signatures of low-surface-density outflowing gas in external galaxies, there have not been resolved observations of outflows in galaxies below the SFMS, *until now*. Recent deep MUSE observations taken as part of MAUVE (see section 2) have revealed, for the first time, anomalous gas likely tracing outflows in the inner parts of heavily stripped satellite galaxies in the Virgo cluster. While, it is unclear whether the Orr et al. (2022b) model can explain observations of outflows in galaxies below the SFMS, the regime of satellites below the SFMS experiencing environmental effects offers rich grounds for exploration of the physics of outflows. Since most of the CGM and ISM are expected to be stripped, the balance between phases, radiation, momentum pressure and cosmic rays would be different from theoretical predictions that do not factor in environmental effects. Further, there is growing evidence supporting the role of feedback in fully quenching satellites and in enhancing the efficiency of environmental quenching mechanisms (e.g. Cortese et al. 2021). However, our understanding of the structure of outflows in galaxies undergoing or having undergone environmental effects remains unexplored. **How does the outflow impact the star formation and the gas distribution in the disc? Can the observed outflows fully quench satellites? Can our current models reconcile observations of outflows in galaxies below the SFMS? Is there a relation between the incidence of outflows and the infall stage?** To fully understand the physics of feedback, we must spatially resolve and systematically characterize the anomalous gas tracing outflows in all phases in a representative sample of nearby galaxies spanning a range of star formation properties and environments.

1.3 Anomalous gas resulting from hydrodynamic interactions with a hot medium

Satellite galaxies infalling into clusters suffer varying degrees of environmental effects depending on factors such as their masses, orbits, and time since first infall. As satellites approach their first pericentre passage, they initially experience a process known as starvation, where gas accretion from the CGM is curtailed (e.g. Balogh et al. 2000). This is followed by the stripping of the outer regions of the ISM through a combination of hydrodynamical (e.g. ram pressure stripping) and/or gravitational quenching mechanisms (see right panel of figure 1). This process typically produces anomalous gas with distinct extended, tail-like morphology trailing from the satellites (see figure 4). The

class of galaxies exhibiting these ram-pressure-stripped tails are commonly referred to as jellyfish galaxies. The trailing tails and truncated asymmetric gas discs typically observed in HI allow us to infer orbits and infall stage of satellites. Such anomalous gas structures have been characterised in the cold neutral phase with HI 21cm (e.g. Lee et al. 2022; Hess et al. 2022; Serra et al. 2024; Boselli et al. 2023), cold molecular phase with CO (e.g. Bacchini et al. 2023), and ionised phase with multiple emission lines (e.g. H α : Bellhouse et al. 2017; Vulcani et al. 2021).

Even though environmental effects can strip most of the gas reservoirs and cease gas inflows, massive satellites ($M_\star > 10^{10} M_\odot$) often retain significant amounts of gas in the inner regions of their discs after their first pericentre passage (e.g. Janowiecki et al. 2020; Cortese et al. 2021). Here, where the environment is less effective, intrinsic quenching mechanisms such as feedback and gas consumption through star formation are expected to dominate (as discussed in subsection 1.2). Therefore, investigating gas flows across physical scales spanning the ISM and CGM is crucial for understanding how different mechanisms regulate star formation and drive galaxy evolution. However, this task is challenging both observationally and in simulations, as gas flows cycle through multiple phases and are influenced by various factors such as gas phase (e.g. Kim et al. 2020), position relative to the star-forming disc (e.g. Nelson et al. 2021), and the properties of the galaxy (e.g. Fielding et al. 2018; Orr et al. 2022a) and its environment (e.g. Aldás et al. 2024). **Are the properties of the anomalous gas consistent across the disc? How do the internal and environmental mechanisms affect the different gas phases in satellites at various infall stages?**

1.4 Anomalous gas resulting from galaxy-galaxy interactions

Interactions can trigger star formation, alter galaxy morphologies, drive non-circular flows, and transport gas away from or into the ISM. Anomalous gas resulting from interactions exhibits distinct morphological and kinematic signatures such as tidal tails, bridges, warps, and extended gas discs. These structures have been observed in the cold neutral phase with HI 21cm (e.g. Sancisi et al. 2008), cold molecular phase with CO (e.g. Brunetti et al. 2024), and ionised phase with multiple emission lines (e.g. H α : Font et al. 2011 MgII: Leclercq et al. 2022). This type of anomalous gas can indicate both gas removal and supply depending on the interaction properties, leading to quenching and starbursts, respectively. Thus, **careful evaluation of the interaction properties is required to understand the origin, fate, and impact of the anomalous gas arising from different types of galaxy-galaxy interactions.** However, decoding interaction properties from observed gas structures requires detailed dynamical modelling and characterisation of the environment (e.g. Sankar et al. in prep). Due to its complexity, this has only been achieved for a small number of interactions with relatively simple configurations. Most notably the interactions between the Magellanic clouds and the Milky Way will supply significant amounts of

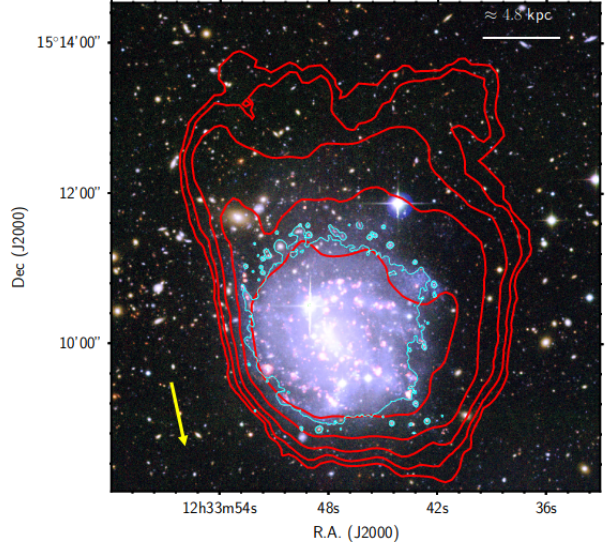


Figure 4: Pseudo-color image of NGC 4523 with HI contours corresponding to column densities of $N(\text{HI}) - 2^n \times 3.9 \times 10^{19} \text{ cm}^{-2}$ overlaid in red. Image taken from Boselli et al. (2023).

cold gas to fuel future star formation episodes in the Milky Way (e.g. Putman et al. 2012). In contrast, interactions in compact groups are expected to result in the quenching of star formation in the resulting merger remnant (e.g. Verdes-Montenegro et al. 2001). **There is a dearth of systematic studies that leverage dynamical models and sensitive observations to investigate anomalous gas resulting from known interaction configurations. Can we detect the evolution of anomalous gas features by observing different stages of similar interaction configurations?**

2 MAUVE

To understand the relative roles of internal and environmental mechanisms in fully quenching satellites, we must connect the multi-phase, multi-scale gas in the ISM and the inner CGM with ongoing star formation in the central regions of galaxies at various stages of infall. Until now, a key missing element has been a multi-wavelength sample of satellites that provides sub-kpc resolution in the central regions and high-resolution sampling of gas extending to the inner CGM.

The Virgo cluster is the nearest and best-studied cluster, with the neutral gas in 53 galaxies and molecular gas in 51 galaxies mapped by VIVA (VLA Imaging of Virgo in Atomic gas; Chung et al. 2009) and VERTICO (Virgo Environment Traced in CO; Brown et al. 2021) respectively at spatial resolutions of ~ 1.5 kpc and ~ 650 pc. The infall stages of satellites in Virgo are also well-characterised through accurate orbital reconstructions and analysis of their gas disc morphologies (e.g. Chung et al. 2009; Yoon et al. 2017). This makes Virgo the ideal cluster for follow-up resolved observations.

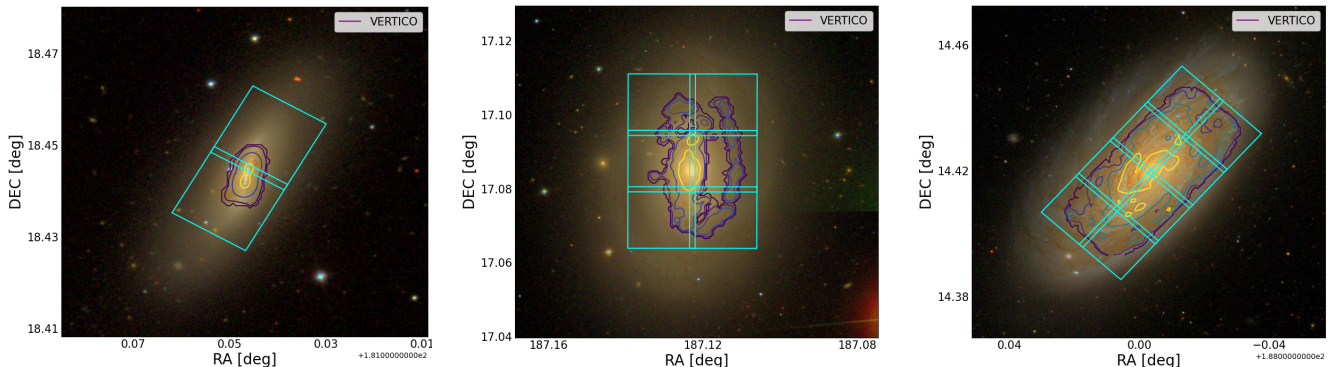


Figure 5: MAUVE footprints and CO contours from VERTICO (Brown et al., 2021) overlaid on optical images for NGC 4064, NDC 4450 and NGC4501 respectively from left to right.

MUSE and ALMA Unveiling the Virgo Environment (MAUVE¹) is a new large program on the European Southern Observatory's (ESO) Very Large Telescope (VLT) in Cerro Paranal, Chile (Watts et al., 2024) that began in Jan 2023. This ongoing program uses the Multi Unit Spectroscopic Explorer (MUSE) instrument to map, at sub-kpc resolutions, the ionised hydrogen and metals across the inner discs of 40 late-type galaxies at various stages of infall into the Virgo cluster. MAUVE will provide valuable information on the star formation properties and the kinematics, morphologies, and chemical properties of the ionised gas at $\sim 100 - 200$ pc spatial scales. Additionally, the ViCTORIA (Virgo Cluster multi Telescope Observations in Radio of Interacting galaxies and AGN; Boselli

¹<https://mauve.icrar.org>

(et al. 2023) project will map the Virgo cluster at HI 21 cm line and 1.4 GHz radio continuum using MeerKAT and at 144 GHz radio continuum using the Low Frequency Array (LOFAR). Together, MAUVE and ViCTORIA will produce the first multi-wavelength sample of satellites, offering sub-kpc resolutions of the gas and star formation in their central regions and \sim kpc resolutions of the neutral hydrogen. This rich dataset of multi-phase gas will enable investigations of the effects of past, ongoing, and future quenching mechanisms at different regions within the satellites. This will, for the first time, allow us to connect gas flows and star-formation properties with internal and external quenching mechanisms as a function of infall time. As discussed above, anomalous gas can provide insights into the relative impacts of intrinsic and environmental mechanisms in fully quenching satellite galaxies. But a suitable sample has been missing **until now**.

3 This work

For my PhD, I will investigate resolved multi-phase gas flows within a sample of satellites in the Virgo cluster, examining their relationship to galaxy properties, infall stage, and the Virgo environment. Utilizing high-resolution data from state-of-the-art instruments such as MUSE, ALMA, and MeerKAT, I will search for anomalous gas in ionized, molecular, and cold phases. My research will involve the first comprehensive census of anomalous gas across a representative sample of galaxies, each experiencing a gamut of secular and environmental evolutionary processes. This will allow us to extract reliable constraints for theoretical frameworks of gas flows. I will validate the observational insights by comparing them with high-resolution mock observations. This work aims to enhance our understanding of the connection between gas flows and star formation in galaxies undergoing environmental quenching. The main questions that I will address are

1. How do the properties of anomalous gas depend on galaxy properties such as star formation rate? Do the properties of anomalous gas evolve with infall time?
2. Are the properties of anomalous gas consistent across all phases? How do the different phases and scales of anomalous gas relate to one another?
3. How do the parameters of outflows change with the infall stage? Does ram pressure stripping make it easier to eject gas out of the disc?

These questions will be split across a series of planned projects each expected to culminate in a journal paper by the end of my PhD.

1. Paper I: Technical paper on the method that I am developing to extract ionised anomalous gas. We will demonstrate the method through application to a sub-sample of MAUVE. Here, I will focus on characterising ionised anomalous gas in first 5 MAUVE galaxies.
2. Paper II: Characterising the ionised anomalous gas in the MAUVE sample and extending the method to include other emission lines (e.g. [NII], CO, HI). In this work, in addition to the ionised anomalous gas characterised in the previous project, I will extend the method to other phases and datasets (e.g. ViCTORIA).

- Paper III: Characterizing gas flows in multi-phase mock observations of high-resolution simulations and exploring the properties of anomalous gas as a function of infall time. In this work, I will examine timescales and pathways of gas depletion and full quenching.

4 Anomalous gas characterisation workflow

We fit multiple Gaussian components to each spaxel of the MUSE H α cubes, identify the rotating component by comparing it to a 3D tilted ring model, and extract a 3D cube of any anomalous gas present. To recover reliable multi-component Gaussian models for every spaxel of a high-resolution emission-line dataset, we must consider spatial coherence, optimal model selection, effects of initial guesses, non-uniform noise properties, and most importantly, systematics introduced by the resolution. In our approach, we favour reliability over completeness to ensure that the anomalous gas model cubes we extract are free from contaminants such as spurious second components, artefacts from data reduction, residual continuum and smeared emission.

In section 4.1, we describe the 2-step 3D tilted ring modelling we implement using ^{3D}BAROLO (Di Teodoro & Fraternali, 2015) to extract the geometry and kinematic parameters of the disc. In 4.2, we briefly discuss important constraints we adopt to perform 3-phase automated Gaussian decomposition using GAUSSPY+ (Riener et al., 2019). Finally in section 5.1, we discuss the 3-step reliability filtering we apply to extract reliable, spatially coherent secondary components.

4.1 Modelling the kinematics of the disc

We use ^{3D}BAROLO to perform 3D tilted ring modelling to extract the geometry and kinematics of concentric annuli that sample the disc. For each ring, ^{3D}BAROLO builds several artificial 3D models, degrades the model to the spatial and spectral resolution of the observation and then performs pixel-by-pixel comparisons between the degraded model and the input data until the best fitting set of geometric and kinematic parameters is obtained. We note that dynamical structures in the disc including lopsidedness, bars, spiral arms, warps, and non-circular motions can often lead to drastic variations in ϕ and i across rings (Di Teodoro & Fraternali, 2015). Fitting the geometrical and kinematic parameters simultaneously can lead to unphysical discontinuities in the derived rotation curve. To rectify this, once the first set of model parameters is fitted, ^{3D}BAROLO interpolates and regularizes the parameters by fixing a functional form. This two-stage fitting regularizes the geometric parameters before fitting the kinematic parameters. In addition to the two-stage fitting in ^{3D}BAROLO, we employ a two-step modelling approach similar to Di Teodoro & Peek (2021) wherein the geometric and kinematic parameters are fitted in the first and second steps respectively. In the first step, the inclination (i), position angle (ϕ), the centre of the rings ((x_θ , y_θ), V_{sys}), rotation velocity (V_{rot}), and velocity dispersion (σ_{gas}) are fitted as free parameters in each ring. In this step, the model is normalised to the azimuthally averaged flux in each ring to fit reliable functional forms to inclination and position angle. In the second step, the rotation and dispersion velocity are fitted as free parameters while all the other parameters are fixed to their respective functions recovered in the first step. In this step, a pixel-by-pixel normalisation is adopted to allow for a non-axisymmetric model in density. In all the steps, we assume a constant scale height of $\sim 200 - 300$ pc and that the disc follows a sech^2 profile. We also adopt a weighting function of $|\cos^2 \theta|$, to give more weight to the pixels near the major axis, where most of the information about rotation velocity and warps reside (Di Teodoro & Peek, 2021).

4.2 Gaussian decomposition

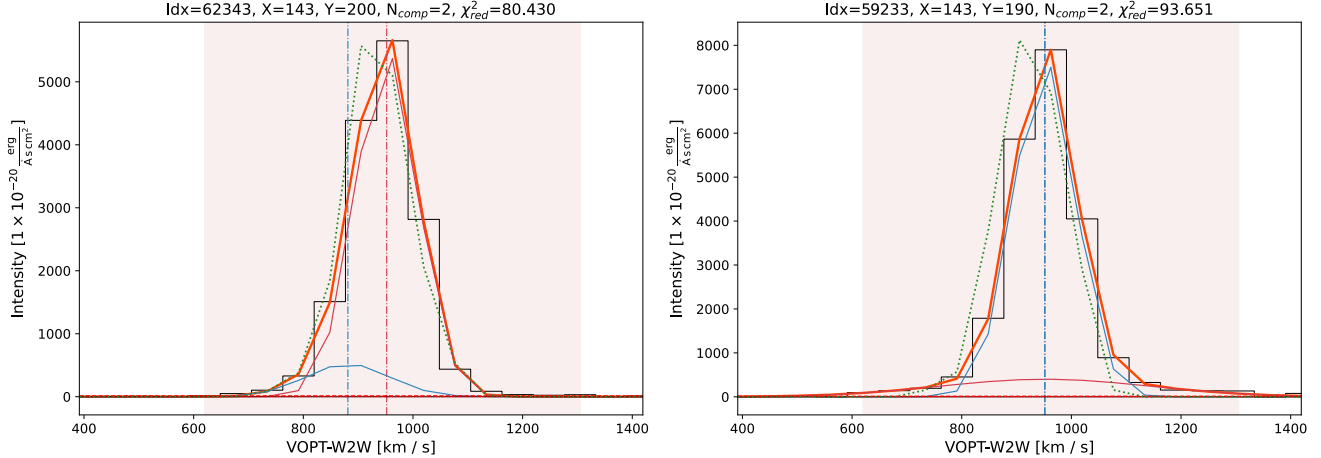


Figure 6: Spectra to illustrate the 2-component Gaussian fitting. The data is plotted in black. Orange and blue solid lines denote primary and secondary fitted model components respectively. The red and blue vertical dash-dotted lines denote the centroid of the respective component. The solid red line denotes the combined Gaussian model. The dotted green line is the tilted ring disc model obtained using 3D BAROLO. The horizontal red dashed line represents the $3\sigma_{RMS}$ level.

We use GAUSSPy+ (Riener et al., 2019) to perform automated physically-motivated Gaussian decomposition for each spaxel of a spectral cube. GAUSSPy+ improves upon the machine-learning-based fitting algorithm, GAUSSPy (Lindner et al., 2015) by including (i) automated preparatory steps for noise calculation and training set creation from the input data; (ii) automated quality checks for the decomposition results; and (iii) automated routines that check the spatial coherence of the decomposition and in case of conflicts, attempts to refit the spectrum based on the models of the neighbouring spaxels. In the preparatory steps, broad features and noise spikes are masked before an RMS noise is extracted per spectra. In the zeroth phase, the package employs derivative spectroscopy to determine initial guesses for the Gaussian components to be fitted. This technique finds the functional maxima and minima of the spectrum using higher-order derivative tests. This is followed by two refitting phases that account for spatial coherence. The first phase of spatially coherent refitting checks for local spatial coherence to account for the Point Spread Function (PSF) and attempts to refit spectra that differ from their immediate neighbours. Here we can specify allowed 'jumps' in the number of components relative to neighbouring spectra (individual and median). In the second phase, a weighting scheme is used to enforce a global form of spatial coherence, wherein, the entire dataset is checked for consistency between the centroid velocities of components in neighbouring spectra. Refitting iterations are then performed for all the flagged spectra. In cases where multiple models can be used to describe a spectrum, χ^2_{red} cannot be used to discern between the models, as the degrees of freedom cannot be reliably estimated in such cases of non-linear models. GAUSSPy+ utilizes the corrected Akaike Information Criterion (AICc) for model selection, which penalises the use of a large number of fit components that do not contribute to a significant increase in fit quality (see equations 9 and 10 in Riener et al. 2019). In figure 6, we show multi-component Gaussian models recovered for two illustrative spectra. The main component aligns with the 3D BAROLO model of the tilted disc (green dotted) and the contiguous secondary component is expected to trace anomalous gas.

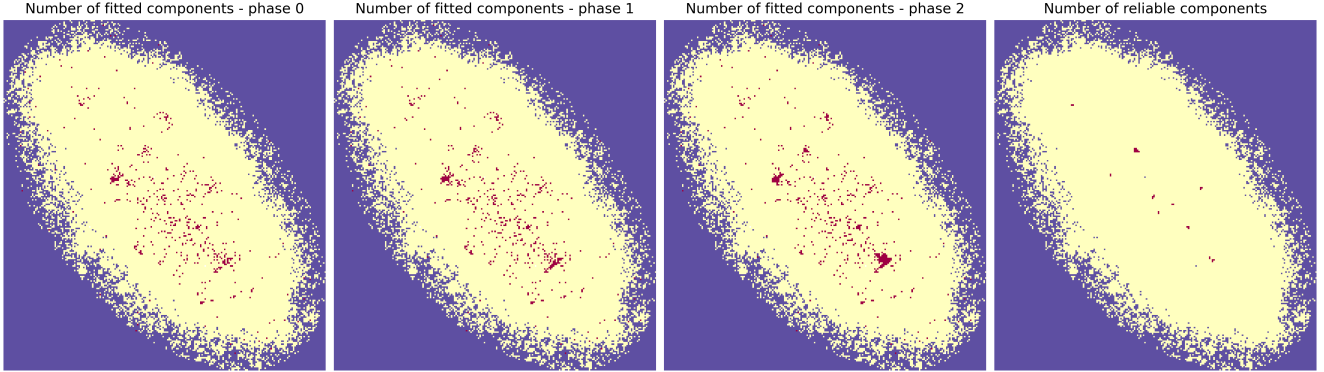


Figure 7: Component maps at each stage of the fitting for IC3392 with $0.2''$ (~ 25 pc) spatial scale. Yellow indicates a single component and red indicates 2 components. Phases 1 and 2 attempt to enforce spatial coherence (panels 2 and 3). Panel 4 shows the component map after 3 steps of reliability filtering.

5 Testing the technique on IC3392

We use IC3392 to test our approach as this heavily stripped backsplash galaxy is least likely to have anomalous gas and visual inspection did not reveal regions with complex kinematic structure. From the continuum subtracted native resolution cube of IC3392, we extract an H α cube that spans ~ 20 spectral channels with a channel separation of ~ 57 kms $^{-1}$ and a pixel scale of $0.2''$. We apply an elliptical spatial mask to exclude noisy regions in the outskirts of the cube. For tilted ring modelling, we input initial guesses for the inclination, position angle, and centre from [Brown et al. \(2021\)](#). In figure 7, we show the component maps recovered from each fitting phase. For IC3392, we obtain about ~ 530 spectra with multiple components out of $\sim 27K$ fitted spectra. But upon inspection, we found that most of the components recovered were unreliable.

5.1 Reliability filtering

Even though GAUSSPY+ performs numerous quality checks, the decomposed spectra still contain spurious multi-component models that will contaminate our analysis. Furthermore, due to the coarse spectral sampling, most multi-component models we obtain have a blended component structure. We can reliably identify secondary components detected with sufficient SNR as anomalous gas if they either have sufficient velocity offset from the primary component or if they have broader FWHM than the primary component. Conventionally, broad H α components have been interpreted as eDIG. While these components can often have velocity centroids similar to that of the primary narrow component, they must, by definition, have broader FWHM than that of the primary component. Thus, blended components must meet certain conditions to be reliable. We are currently testing various reliability diagnostics and we list here those that seem promising. But it is still unclear whether these diagnostics will work on a galaxy with anomalous gas. For IC3392, we apply three reliability filters: (i) SNR filter, (ii) spurious component filter, and (iii) spatial contiguity filter. In the two panels of figure 8 we show the first two reliability filters that we apply to eliminate spurious secondary components.

In panel 1, we plot the peak SNR of the secondary component against the absolute velocity centroid difference between the primary and secondary components. We eliminate all secondary components with a peak SNR equal to

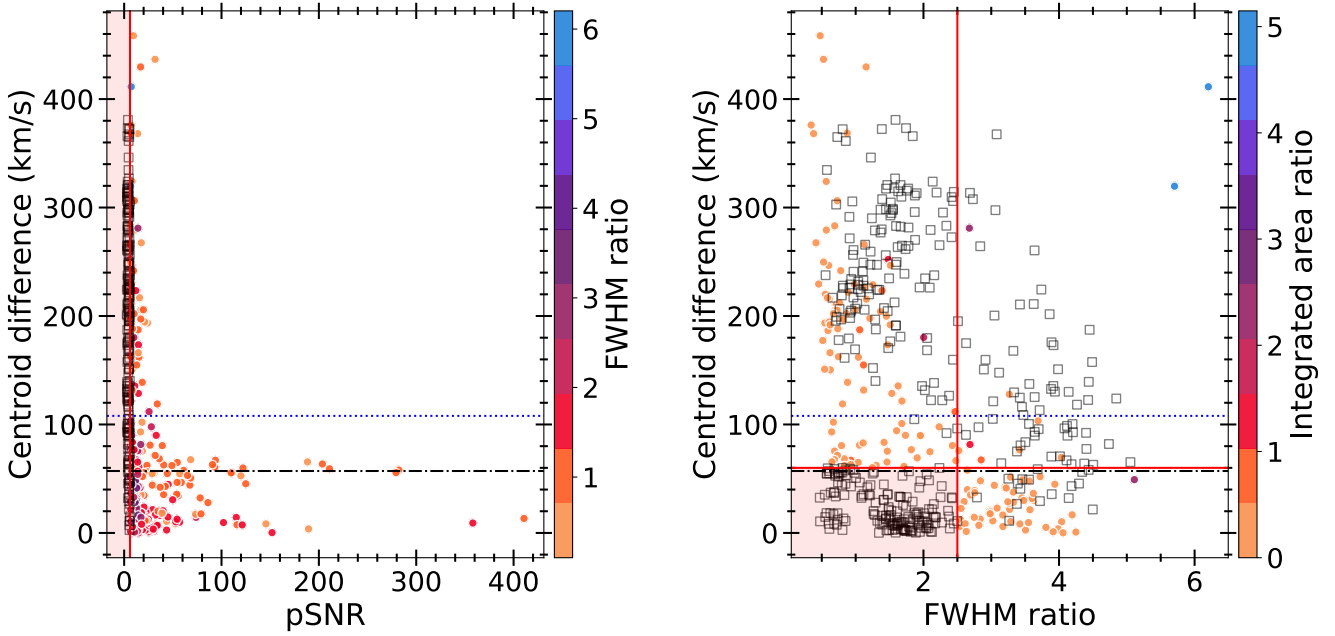


Figure 8: The diagnostic plots used to discard spurious second components. The black unfilled squares show the positions of the discarded components in the parameter spaces plotted. In the first panel, all components with a peak SNR lower than or equal to 6 (red vertical line) are discarded. In the second panel, all components with an integrated ratio less than or equal to 12% are discarded. We also discard spurious components that occupy the third quadrant defined by the channel separation and an FWHM ratio of 2.5. The blue dotted line indicates the spectral resolution.

or lower than 6. We adopt this value after testing a range of thresholds between 3 and 10. After applying the first filter we retain about 300 secondary components. Upon inspecting the filtered set of decomposed profiles of IC3392, we find spurious components which either have low amplitudes and narrow FWHM or centroid velocities and FWHM values that are comparable to the primary component. It is clear from examining the profiles that these spurious components are not required to fit the observed profile. These could either be due to the data quality or the fitting procedure. False component structures can be introduced by artefacts in the spectra such as non-Gaussian noise, residual continuum, inaccurate sky subtraction, or asymmetry due to coarse spectral sampling. The fitting could also yield inaccurate component structures due to attempted fits to non-gaussian residuals and enforced spatial coherence. To discard these, we plot the centroid difference against the FWHM ratio between the secondary and the primary as shown in panel 2 of figure 8. Secondary components with centroid velocities within 60 km s^{-1} from that of the primary component and an FWHM less than 2.5 times that of the FWHM of the primary component are flagged as spurious and discarded. The adopted centroid difference threshold is the channel separation of the cube. The FWHM ratio threshold was adopted after testing a range of values from 1.0 to 3.0. In panel 2 of figure 8, the spurious components occupy the third quadrant defined by the red orthogonal lines denoting the imposed thresholds. After applying the first and second reliability filters, we retain about 100 secondary components. For a secondary component to be considered physical, it must be spatially contiguous, meaning it should be detected in adjacent spaxels as well. To ensure this, we apply a third reliability filter that checks for spatial contiguity among adjacent spaxels. Specifically, this filter requires that a reliable multi-component model must have at least one additional reliable counterpart within its 8 contiguous spaxels. We retain 32 secondary components in IC3392 after applying the contiguity filter.

6 Next steps

In summary, after 3 phases of fitting over 27K H α spectra, we obtained about 530 multi-component models in IC3392. We are currently favouring a 3-step reliability filtering technique to extract reliable, contiguous secondary components from the decomposition results. Applying these filters to IC3392 yields only 32 secondary components. As expected, this does not allow us to make physical inferences about anomalous gas in IC3392. We list our next steps below.

1. Test the reliability filters on the first five galaxies in MAUVE with plausible hints of anomalous gas.
2. Develop a tagging technique to identify the disc and anomalous gas components.
3. Explore rebinning to see if the fraction of reliable anomalous gas components recovered improves.

Supervision

- Principal Supervisor (80%) – Prof. Barbara Catinella

Prof. Catinella and I will have weekly meetings to discuss my progress and future work. I will also take part in group meetings managed by Prof. Catinella and Prof. Cortese. Additionally, if required, we will meet with Prof. Catinella's wider international collaborations.

- Co-Supervisor (20%) – Prof. Chris Power

Prof. Power and I will meet as needed for the beginning of my PhD, and transition to weekly as my research becomes more numerically focused.

References

- Afruni A., Fraternali F., Pezzulli G., 2021, [Monthly Notices of the Royal Astronomical Society](#), 501, 5575
Afruni A., Pezzulli G., Fraternali F., Grønnow A., 2023, [Monthly Notices of the Royal Astronomical Society](#), 524, 2351
Aldás F., Gómez F. A., Vega-Martínez C., Zenteno A., Carrasco E. R., 2024, Differences in the Physical Properties of Satellite Galaxies within Relaxed and Disturbed Galaxy Groups and Clusters ([arXiv:2408.05305](#))
Bacchini C., et al., 2023, [The Astrophysical Journal](#), 950, 24
Balogh M. L., Navarro J. F., Morris S. L., 2000, [The Astrophysical Journal](#), 540, 113
Bellhouse C., et al., 2017, [The Astrophysical Journal](#), 844, 49
Boettcher E., Gallagher III J. S., Zweibel E. G., 2017, [The Astrophysical Journal](#), 845, 155
Boettcher E., Gallagher III J. S., Zweibel E. G., 2019, [The Astrophysical Journal](#), 885, 160
Boomsma R., Oosterloo T. A., Fraternali F., van der Hulst J. M., Sancisi R., 2008, [Astronomy and Astrophysics](#), Volume 490, Issue 2, 2008, pp.555-570, 490, 555
Boselli A., et al., 2023, [Astronomy & Astrophysics](#), 676, A92
Brown T., et al., 2021, [The Astrophysical Journal Supplement Series](#), 257, 21

- Brunetti N., et al., 2024, *Monthly Notices of the Royal Astronomical Society*, 530, 597
- Chung A., Van Gorkom J. H., Kenney J. D. P., Crowl H., Vollmer B., 2009, *The Astronomical Journal*, 138, 1741
- Cortese L., Catinella B., Smith R., 2021, *Publications of the Astronomical Society of Australia*, 38, e035
- Di Teodoro E. M., Fraternali F., 2015, *Monthly Notices of the Royal Astronomical Society*, 451, 3021
- Di Teodoro E. M., Peek J. E. G., 2021, *The Astrophysical Journal*, 923, 220
- Fielding D. B., Bryan G. L., 2022, *The Astrophysical Journal*, 924, 82
- Fielding D., Quataert E., Martizzi D., 2018, *Monthly Notices of the Royal Astronomical Society*, 481, 3325
- Font J., et al., 2011, *The Astrophysical Journal*, 740, L1
- Fraternali F., 2017, in Fox A., Davé R., eds, *Astrophysics and Space Science Library, Gas Accretion onto Galaxies*. Springer International Publishing, Cham, pp 323–353, doi:10.1007/978-3-319-52512-9_14
- Fraternali F., van Moorsel G., Sancisi R., Oosterloo T., 2002, *The Astronomical Journal*, 123, 3124
- Fraternali F., Oosterloo T., Sancisi R., 2004, *Astronomy and Astrophysics*, v.424, p.485-495 (2004), 424, 485
- Fraternali F., Oosterloo T. A., Sancisi R., Swaters R., 2005, 331, 239
- Hess K. M., Kotulla R., Chen H., Carignan C., Gallagher J. S., Jarrett T. H., Kraan-Korteweg R. C., 2022, *Astronomy and Astrophysics*, 668, A184
- Janowiecki S., Catinella B., Cortese L., Saintonge A., Wang J., 2020, *Monthly Notices of the Royal Astronomical Society*, 493, 1982
- Kim C.-G., et al., 2020, *The Astrophysical Journal*, 903, L34
- Leclercq F., et al., 2022, *Astronomy & Astrophysics*, 663, A11
- Lee S., Sheen Y.-K., Yoon H., Jaffé Y., Chung A., 2022, *Monthly Notices of the Royal Astronomical Society*, 517, 2912
- Li M., Bryan G. L., 2020, *The Astrophysical Journal*, 890, L30
- Li A., Fraternali F., Marasco A., Trager S. C., Pezzulli G., Piña P. E. M., Verheijen M. A. W., 2023, Fountain-Driven Gas Accretion Feeding Star Formation over the Disc of NGC 2403 (arXiv:2301.03614)
- Lindner R. R., et al., 2015, *The Astronomical Journal*, 149, 138
- Marasco A., et al., 2019, *Astronomy & Astrophysics*, 631, A50
- Nelson D., Byrohl C., Peroux C., Rubin K. H. R., Burchett J. N., 2021, *Monthly Notices of the Royal Astronomical Society*, 507, 4445
- Oosterloo T., Fraternali F., Sancisi R., 2007, *The Astronomical Journal*, 134, 1019
- Orr M. E., Fielding D. B., Hayward C. C., Burkhardt B., 2022a, *The Astrophysical Journal*, 924, L28
- Orr M. E., Fielding D. B., Hayward C. C., Burkhardt B., 2022b, *The Astrophysical Journal*, 932, 88
- Putman M. E., Peek J. E. G., Joung M. R., 2012, *Annual Review of Astronomy and Astrophysics*, 50, 491
- Reichardt Chu B., et al., 2022, *The Astrophysical Journal*, 941, 163
- Reichardt Chu B., et al., 2024, DUVET: Sub-Kiloparsec Resolved Star Formation Driven Outflows in a Sample of Local Starbursting Disk Galaxies, doi:10.48550/arXiv.2402.17830
- Riener M., Kainulainen J., Henshaw J. D., Orkisz J. H., Murray C. E., Beuther H., 2019, *Astronomy & Astrophysics*, 628, A78
- Sancisi R., Fraternali F., Oosterloo T., van der Hulst T., 2008, *The Astronomy and Astrophysics Review*, Volume 15, Issue 3, pp.189-223, 15, 189
- Schneider E. E., Ostriker E. C., Robertson B. E., Thompson T. A., 2020, *The Astrophysical Journal*, 895, 43
- Serra P., et al., 2024, The MeerKAT Fornax Survey. III. Ram-pressure Stripping of the Tidally Interacting Galaxy NGC 1427A in the Fornax Cluster (arXiv:2407.09082)

- Stern J., Fielding D., Hafen Z., Su K.-Y., Naor N., Faucher-Giguère C.-A., Quataert E., Bullock J., 2024, [Monthly Notices of the Royal Astronomical Society](#)
- Thompson T. A., Heckman T. M., 2024, Theory and Observation of Winds from Star-Forming Galaxies ([arXiv:2406.08561](#))
- Tumlinson J., Peeples M. S., Werk J. K., 2017, [Annual Review of Astronomy and Astrophysics](#), 55, 389
- Veilleux S., Maiolino R., Bolatto A. D., Aalto S., 2020, [Astronomy and Astrophysics Review](#), 28, 2
- Verdes-Montenegro L., Yun M. S., Williams B. A., Huchtmeier W. K., Del Olmo A., Perea J., 2001, [Astronomy and Astrophysics](#), v.377, p.812-826 (2001), 377, 812
- Vulcani B., et al., 2021, [The Astrophysical Journal](#), 914, 27
- Watts A. B., et al., 2024, MAUVE: A 6 Kpc Bipolar Outflow Launched from NGC 4383, One of the Most HI-rich Galaxies in the Virgo Cluster ([arXiv:2404.12616](#))
- Whitaker K. E., van Dokkum P. G., Brammer G., Franx M., 2012, [The Astrophysical Journal](#), 754, L29
- Yoon H., Chung A., Smith R., Jaffé Y. L., 2017, [The Astrophysical Journal](#), 838, 81

